



UNIVERSITY OF LEEDS

This is a repository copy of *Tree species richness and diversity predicts the magnitude of urban heat island mitigation effects of greenspaces*.

White Rose Research Online URL for this paper:

<https://eprints.whiterose.ac.uk/170137/>

Version: Accepted Version

Article:

Wang, X, Dallimer, M orcid.org/0000-0001-8120-3309, Scott, CE orcid.org/0000-0002-0187-969X et al. (2 more authors) (2021) Tree species richness and diversity predicts the magnitude of urban heat island mitigation effects of greenspaces. *Science of The Total Environment*, 770. 145211. ISSN 0048-9697

<https://doi.org/10.1016/j.scitotenv.2021.145211>

© 2021 Elsevier B.V. All rights reserved. This manuscript version is made available under the CC-BY-NC-ND 4.0 license <http://creativecommons.org/licenses/by-nc-nd/4.0/>.

Reuse

This article is distributed under the terms of the Creative Commons Attribution-NonCommercial-NoDerivs (CC BY-NC-ND) licence. This licence only allows you to download this work and share it with others as long as you credit the authors, but you can't change the article in any way or use it commercially. More information and the full terms of the licence here: <https://creativecommons.org/licenses/>

Takedown

If you consider content in White Rose Research Online to be in breach of UK law, please notify us by emailing eprints@whiterose.ac.uk including the URL of the record and the reason for the withdrawal request.



eprints@whiterose.ac.uk
<https://eprints.whiterose.ac.uk/>

1 **Tree species richness and diversity predicts the magnitude of**
2 **urban heat island mitigation effects of greenspaces**

3

4 Xinjun Wang ^{a, b}, Martin Dallimer ^c, Catherine E. Scott ^d, Weiting Shi ^b, Jixi Gao ^{e*}

5

6 ^a Nanjing Institute of Environmental Science, Ministry of Ecology and Environment,
7 Nanjing, Jiangsu, 210042, China

8 ^b Department of Environmental Design, School of Art and Design, Changzhou Institute
9 of Technology, Changzhou, Jiangsu, 213022, China

10 ^c Sustainability Research Institute, School of Earth and Environment, University of
11 Leeds, Leeds LS2 9JT, United Kingdom

12 ^d Institute for Climate and Atmospheric Science, School of Earth and Environment,
13 University of Leeds, Leeds LS2 9JT, United Kingdom

14 ^e Ministry of Ecology and Environment Center for Satellite Application on Ecology and
15 Environment, Beijing, 100094, China

16

17

18 **Abstract**

19 The Urban Heat Island Effect (UHIE) is a widely recognised phenomenon that
20 profoundly affects the quality of life for urban citizens. Urban greenspace can help
21 mitigate the UHIE, but the characteristics that determine the extent to which any given
22 greenspace can cool an urban area are not well understood. A key characteristic is likely
23 to be the properties of trees that are found in a greenspace. Here, we explore the
24 sensitivity of the strength of the cooling effect to tree community structure for
25 greenspaces in Changzhou, China. Land surface temperatures were retrieved from
26 Landsat 7 ETM+ and Landsat 8 TIRS and were used to evaluate the temperature drop
27 amplitude (TDA) and cooling range (CR) of 15 greenspaces across each of the four
28 seasons. Tree community structure of the greenspaces was investigated using 156
29 sample plots across the 15 greenspaces. We found that a number of plant community
30 structure indicators of greenspaces have a significant impact on the strength of the
31 cooling effect. The Shannon-Wiener diversity index, tree species richness and tree
32 canopy coverage of greenspaces are all positively correlated with the magnitude of the
33 temperature drop amplitude, with the strength of their influence varying seasonally. We
34 also find that mean crown width is positively correlated with cooling range in summer
35 and autumn, whilst greenspace tree density is negatively correlated with cooling range
36 in winter. Our findings improve understanding of the relationship between plant
37 community structure and the cooling effect of greenspaces. In particular, we highlight
38 the important role that tree species diversity provides for mitigating the UHIE, and
39 suggest that if planners wish to improve the role of urban greenspaces in cooling cities,

40 they should include a higher diversity of trees species.

41

42 **Keywords:** cooling effect, plant community structure, land surface temperature,
43 Shannon-Wiener diversity index, species richness, ecosystem services, tree coverage

44

45 Abbreviations: UHIE, Urban heat island effect; LST, Land surface temperature;
46 DBH, Diameter at breast height; TDA, Temperature drop amplitude; CR, Cooling
47 range

48

49 **1. Introduction**

50 The proportion of the global human population living in towns and cities is
51 projected to reach 66% by 2050, with the majority of this growth occurring in Asia
52 and Africa (United Nations, 2014). The environmental impacts of rapid urbanization
53 have received greater attention and include increased, and more extreme temperatures
54 as part of the Urban Heat Island Effect (UHIE) (Buyantuyev and Wu, 2010; Liu et al.,
55 2009), poor air quality (Fu and Chen, 2017), increased water and energy consumption
56 and poorer health and wellbeing of urban residents (Morris et al., 2017; Santamouris,
57 2020; Yang et al., 2020b).

58 In parallel with this rapid urbanisation, global mean surface temperatures are
59 projected to rise throughout the century, to an extent that depends upon future
60 anthropogenic emissions (IPCC, 2018). The emergence of urban heat islands is one of
61 the key environmental issues of the 21st century (Oke, 1973), not least because rising

62 temperatures associated with global climate change may aggravate the impacts of the
63 UHIE that are already common in urban areas (Luber and McGeehin, 2008), leading
64 to more extreme heat stress, especially in megacities (Argüeso et al., 2015; IPCC,
65 2018).

66 Urbanization changes the reflection and absorption of solar radiation by the
67 Earth's surface, which leads to a higher temperature in urban areas than suburban and
68 rural areas. This difference in temperature has been termed the UHIE (Bowler et al.,
69 2010). The UHIE can profoundly affect the quality of life for urban citizens, with
70 higher temperatures, water use increases, for instance when irrigation is required
71 (Guhathakurta and Gober, 2007; McDonald et al., 2011). Similarly, the demand for
72 living and office spaces to be cooled, through the provision of air conditioning can
73 require more energy (Salvati et al., 2017; Yang et al., 2020b), which leads to higher
74 levels of air pollution. Finally, raised temperatures in cities are associated with an
75 increase in mortality and heat-related health conditions (Boumans et al., 2014; Morris
76 et al., 2017). Mitigating the UHIE has therefore become a core concern for urban
77 sustainability.

78 Urban greenspaces have increasingly been recognized as providing multiple
79 benefits for improving urban sustainability and liveability (Grilo et al., 2020; Shekhar
80 and Aryal, 2019; Verdú-Vázquez et al., 2017). Greenspaces include parks and
81 reserves, sports fields, community gardens, street trees, and nature conservation areas,
82 as well as less conventional spaces such as green walls and green alleyways (Wolch et
83 al., 2014). In terms of the UHIE, greenspaces provide a cooling effect thereby

84 mitigating higher temperatures especially in summer (Bernatzky, 1982; Cao et al.,
85 2010; Chang and Li, 2014; Du et al., 2017; Qiu and Jia, 2020) while a lack of
86 greenspaces is associated with higher temperatures (Luber and McGeehin, 2008).
87 Greenspaces do this in two ways. First, trees and other vegetation can directly shade
88 surfaces and thereby reduce the amount of incident solar radiation (Dimoudi and
89 Nikolopoulou, 2003). Second, greenspaces enable the conversion of incident radiation
90 to latent rather than sensible heat, through transpiration by vegetation (Moss et al.,
91 2019). These effects combine to lower temperatures within greenspaces, compared to
92 the surrounding built-up areas. The cooling effect of greenspaces also extends beyond
93 the edge of the greenspace itself into surrounding streets (Lin et al., 2015).

94 The physical structure of greenspaces can alter their ability to mitigate the UHIE.
95 Size, impervious surface coverage, vegetation coverage and the presence of water
96 have all been shown to correlate with the magnitude of the cooling effect (Du et al.,
97 2017; Li et al., 2011; Lu et al., 2017; Srivanit and Hokao, 2013). The size of
98 greenspaces is positively correlated with the strength of the cooling effect (Vaz
99 Monteiro et al., 2016; Yang et al., 2020a). Further research has focused on threshold-
100 size of greenspaces that is helpful to optimize greenspace's cooling effects (Yu et al.,
101 2020; Yu et al., 2017). However, the requirement to provide more greenspaces is often
102 difficult in cities due to the intense pressure on land for development and construction
103 (Jim, 1998). An alternative approach could be to optimize plant community diversity
104 and structure within greenspaces to maximize any cooling effect and UHIE mitigation
105 (Tang et al., 2017).

106 Plant community structure, such as the number of trees, species composition, tree
107 size, tree canopy cover, tree height, tree location and tree health, all influence
108 ecosystem service provision from greenspaces (Chen et al., 2020; Moser et al., 2015;
109 Nowak, 2008; Zhang et al., 2013). However, not all urban vegetation is equally
110 effective in reducing temperatures. Indeed, tree canopies differ in their ability to
111 intercept and absorb radiation and to transpire (Kelliher et al., 1993). The foliage
112 characteristics and tree's mature shape (for example, canopy geometry and total
113 height) can affect the thermal performance and shade effectiveness (Leuzinger et al.,
114 2010; Shahidan et al., 2010). The particular type of treed habitat has also been shown
115 to have an influence on the cooling effect. For instance, in Singapore, secondary
116 forest was the most efficient in providing cooling. Vegetation in secondary forest was
117 denser than elsewhere, thus preventing more radiation from reaching the forest floor
118 and simultaneously increasing evaporation cooling (Richards et al., 2020). The
119 "forest-like" characteristics of secondary forest, with its complex vertical structure
120 and, by extension, varied species composition might be important. Further, for a range
121 of tree and bamboo species, tree foliage density makes the greatest contribution to the
122 cooling effect, followed by leaf thickness, leaf texture and leaf colour lightness (Bau-
123 Show and Yann-Jou, 2010). Thermal satellite data indicated that every unit increase in
124 leaf area index decreased land surface temperature by 1.2°C (Hardin and Jensen,
125 2007). Canopy density, leaf area index and tree height were the most significant
126 drivers of the magnitude of the cooling effect in Changchun, China (Tang et al.,
127 2017). Multilayer plant communities were the most effective in terms of the cooling

128 effect, and bamboo groves were the least effective (Zhang et al., 2013). Plant
129 community structure has a significant impact on the cooling effect of greenspaces
130 (Petri et al., 2019; Tang et al., 2017; Zhang et al., 2013). Despite this research, thus far
131 the particular contribution of tree diversity to the cooling effect remains poorly
132 explored.

133 The cooling effect of urban greenspaces will vary with the season as vegetation
134 cover, soil moisture, impervious surfaces, air humidity and albedo vary seasonally
135 (Haashemi et al., 2016; Jonsson, 2004). Seasonal variation in correlations between
136 vegetation and LST suggests much stronger coupling during warmer seasons than
137 cooler seasons (Buyantuyev and Wu, 2010). Most of the previous studies have studied
138 the thermal environment relief function of the plant community structure at a specific
139 time, especially in summer (Du et al., 2017; Perini and Magliocco, 2014; Yang et al.,
140 2017). We therefore know relatively little about the seasonal variations of cooling
141 effects in relation to plant community structure.

142 Here we address an important knowledge gap regarding the influence of tree
143 diversity in UHIE mitigation. We use two Landsat datasets (Landsat 8 TIRS and
144 Landsat 7 ETM+) and ground-based tree plots across the rapidly urbanizing city of
145 Changzhou, China. We answer the following three questions that have not previously
146 been adequately addressed: (1) How do the cooling effects of urban greenspaces vary
147 seasonally? (2) What role does tree species diversity play in underpinning the cooling
148 effect?

149

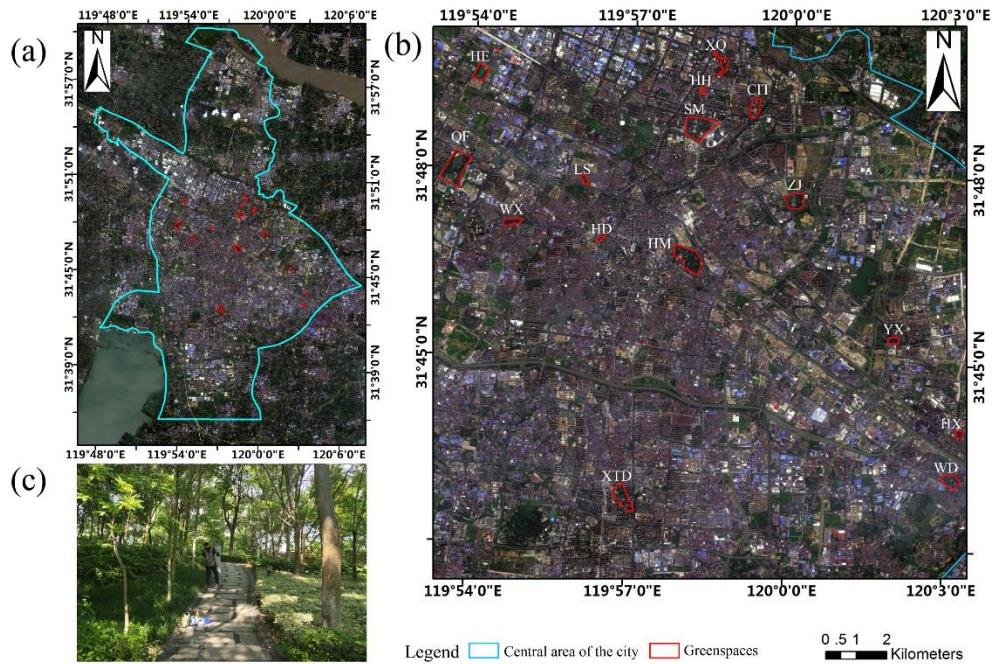
150 2. Materials and methods

151 2.1 Study area

152 Covering 4385 km² Changzhou city, Jiangsu Province, China, is urbanizing
153 rapidly. In 2018, the city had 4,729,000 residents, living at a density of 1079
154 inhabitants/ km² (Changzhou Statistics Bureau, 2019). Changzhou lies in the Yangtze
155 River Delta in the northern subtropical humid area (Zheng et al., 2010), and the
156 seasons are divided into spring, summer, autumn and winter from March to May, June
157 to August, September to November and December to February (Yu et al., 2014). Mean
158 seasonal temperatures for the city between 1952 and 2006 were 14.7°C, 26.7°C,
159 17.5°C and 4.4°C for spring, summer, autumn and winter respectively (Qin et al.,
160 2008). Around 57% of the city is covered in impervious surfaces such as buildings
161 and roads (Changzhou Statistics Bureau, 2019).

162 Based on the 2011-2020 Changzhou City Master Plan (Figure 1, a), the central
163 area is the construction concentration area of Changzhou, which includes the most
164 densely populated and built up region of the city, but also includes greenspaces and
165 infrastructure, as well as canals and rivers. Fifteen publicly accessible greenspaces in
166 the core area of the central city were selected (Figure 1, b). They varied in size, tree
167 canopy cover and tree community composition. Most of these greenspaces were
168 instigated in the last 40 years and are therefore characterised by relatively small trees
169 compared to more established public parks in Europe and North America (Figure 1,
170 c). As public spaces, most of the greenspaces is composed of impervious surfaces,
171 characterised by grassed areas and mixed plantings of deciduous and evergreen tree

172 species. Water bodies are also commonly present.



173 Figure 1 (a) The central area of the city. (b) The location of 15 greenspaces
174 (outlined in red) in the core of centre area of Changzhou, China. (c) The typical plant
175 community in greenspaces of Changzhou. Letters give abbreviated greenspaces
176 names: He=He park, XQ=Xinqu park, HH=Hehai residential area, SM=Shiming
177 square, CIT=Campus of Changzhou institute of technology, QF=Qingfeng Park,
178 WX=Wuxing Park, LS=Lushu park, HD=Huaide square, HM=Hongmei park,
179 ZJ=Zijing Park, YX=Yuxiu park, XTD=Xintiandi park, HX=Huaxi park,
180 WD=Weidun park.

181

182 2.2 Data sources and processing

183 2.2.1 Data sources

184 Land surface temperatures collected from remote sensing thermal infrared
185 images are positively correlated with air temperatures (Ren et al., 2016). In this study,

186 we therefore used Landsat images of the study area to measure temperature across all
187 four seasons in 2017-2018. To achieve better results for the retrieved land surface
188 temperatures, four cloudless remote images were selected from Landsat datasets at
189 Row/Path: 38/119. Two Landsat 8 TIRS images covered winter (21 December 2017
190 GMT: 02:31:23) and spring (27 March 2018, GMT: 02:30:40). Two Landsat 7 ETM+
191 images were used for summer (07 June 2018, GMT: 02:31:02) and autumn (29
192 October 2018, GMT: 02:28:05). In all cases cloud cover was <10%, images covered
193 daytime and were download from <https://glovis.usgs.gov/>. The lowest and highest air
194 temperature corresponding to the day of remote sensing images are 13°C~25°C (27
195 March 2018) as spring, 22°C~31°C (7 June 2018) as summer, 11°C~23°C (29
196 October 2018) as autumn and 1°C~11°C (21 December 2017) as winter.

197

198 **2.2.2 Estimating land surface temperatures**

199 We calculated land surface temperature (LST) based on a previously validated
200 radiative transfer equation (Du et al., 2017; Masoudi and Tan, 2019; Qiu and Jia,
201 2020; Wang et al., 2018). Land surface emissivity (ϵ) is an essential parameter for
202 retrieving LST from thermal infrared remote sensing data. The land surface can be
203 viewed as composed of three land cover patterns: vegetation, bare soil and water (Qin
204 et al., 2004). Land surface emissivity (ϵ) is estimated by using the values of NDVI
205 and green cover ratio (P_v):

$$206 \quad P_v = [(NDVI - NDVI_{soil}) / (NDVI_{veg} - NDVI_{soil})] \quad (1)$$

207 Where NDVI is normalized difference vegetation index, $NDVI_{soil}$ and $NDVI_{veg}$

208 are NDVI in bare land and vegetation area, set as 0.05 and 0.7, respectively.

209 Based on the land cover patterns, $\varepsilon_{\text{water}}$ (the Land surface emissivity of water) is
210 0.995.

$$211 \quad \varepsilon_{\text{vegetation}} = 0.9625 + 0.0614P_v - 0.0461P_v^2 \quad (2)$$

$$212 \quad \varepsilon_{\text{building}} = 0.9589 + 0.086P_v - 0.0671P_v^2 \quad (3)$$

213 where $\varepsilon_{\text{vegetation}}$ is the emissivity of the natural surface, $\varepsilon_{\text{building}}$ is the emissivity of
214 the built surface (Qin et al., 2004; Shi and Zhang, 2018).

$$215 \quad B(T_s) = [L_\lambda - L^\uparrow - \tau(1 - \varepsilon)L^\downarrow] / \tau\varepsilon \quad (4)$$

216 L_λ is the radiance registered by the sensor, $B(\text{Loreau et al.})$ is the blackbody
217 radiance related to the surface temperature by Planck's law, L^\uparrow and L^\downarrow are the upward
218 and downward atmospheric radiance, respectively, τ is the atmospheric transmission.

$$219 \quad T_s = K_2 / \ln[K_1 / B(T_s) + 1] \quad (5)$$

220 T_s is the LST, calculated by Planck formula, for band 10 of TIRS, $K_1 = 774.89$
221 $\text{W}/(\text{m}^2 \cdot \mu\text{m} \cdot \text{sr})$, $K_2 = 1321.08 \text{ K}$; for band 6 of ETM+, $K_1 = 666.09 \text{ W}/(\text{m}^2 \cdot \mu\text{m} \cdot \text{sr})$,
222 $K_2 = 1282.71 \text{ K}$ (Yu et al., 2017). Atmospheric profile parameters (L^\uparrow , L^\downarrow , and τ) can
223 be obtained by entering the imaging time and the centre coordinate by latitude: 31.48,
224 longitude: 119.53 on the website provided by NASA (<http://atmcorr.gsfc.nasa.gov/>).

225 These data allow us to calculate the LST for each greenspace and each season, as well
226 as the mean LST for the central area of the city (Fig. 2).

227

228 **2.2.3 Metrics of cooling effects**

229 The cooling effect of urban greenspaces is evaluated by quantifying the

230 difference in LST between a greenspace and the surrounding built area. There are
231 several metrics which can be used for this (Du et al., 2017; Sun et al., 2012; Yang et
232 al., 2020a). Here we used the cooling range and temperature drop amplitude. The
233 cooling range is defined as the distance from the greenspace boundary at which the
234 first turning point in LST occurs (Du et al., 2017; Qiu and Jia, 2020). The turning
235 point of an LST curve was identified by piecewise regression as the point where the
236 slope of LST curve changes sharply. To estimate the cooling range, we calculated the
237 mean LST within 15 m buffers around each greenspace. TDA is the temperature
238 difference between the mean LST of the greenspace and the mean LST at the cooling
239 range (Figure 3).

240

241 **2.2.4 Urban greenspace tree community structure**

242 We followed the i-Tree Eco protocol (i-Tree, 2020), which generates sample plot
243 locations across a survey area in order to achieve a standard error of 12% for
244 estimates of the total number of trees present (Martin et al., 2013). In addition to the i-
245 Tree Eco protocol, to ensure we captured variation in tree community structure, we
246 constrained plot site selection so that no portion of any plots fell on water or sealed
247 surface, and that plots were not clustered in small areas of larger greenspaces. Each
248 plot was approximately 400 m² (a circle with an 11.34 m radius). The plot selection
249 process resulted in 156 sample plots within our study greenspaces, which sampled
250 62400 m² from the total unsealed surface land area of the 15 greenspaces of 1300341
251 m² (Appendix 1). Within each plot we identified each tree to species, recorded its

252 height, diameter at breast height (1.37 m above ground, DBH), crown width, crown
253 height, crown health, crown base height, as well as the total number of trees in each
254 plot. Every tree with diameter greater than 4 cm was measured (Table 2). Data were
255 collected between June 2017 and February 2018. We further calculated the tree
256 coverage of each greenspace by using i-Tree Canopy (i-Tree Canopy, 2020) in which
257 tree coverage is assessed by a random sample of Google Maps aerial photography. In
258 i-Tree Canopy, sample points are generated randomly, and pre-defined cover types
259 can be chosen for the sample points. We evaluated between 300 and 1000 sample
260 points in each greenspace, with the number of points proportional to greenspace area.

261 We calculated two metrics of tree diversity, namely species richness (i.e., the
262 number of species) and the Shannon-Wiener diversity index which combines species
263 richness and the relative frequency of these species (evenness), as per equation (6).

$$273 \quad H' = - \sum_{i=1}^s p_i \ln(p_i) \quad (6)$$

264 Where p_i is the relative frequency of species i in the community and S is the number
265 of species. Species richness is the number of different species in a community. In this
266 study, large-sized greenspaces have more sample plots than small-sized greenspaces,
267 so we calculate *richness per plot* as an indicator of the richness to account for the
268 relationships that exist between sampled area and species richness. We wished to
269 understand the strength of the relationship between tree diversity and the cooling
270 effects of urban greenspaces, taking into account the role of tree community structure.
271 We did this in two stages. Firstly, we used correlations (Pearson's or Spearman's
272 correlation coefficient depending on whether specific data were normally distributed)

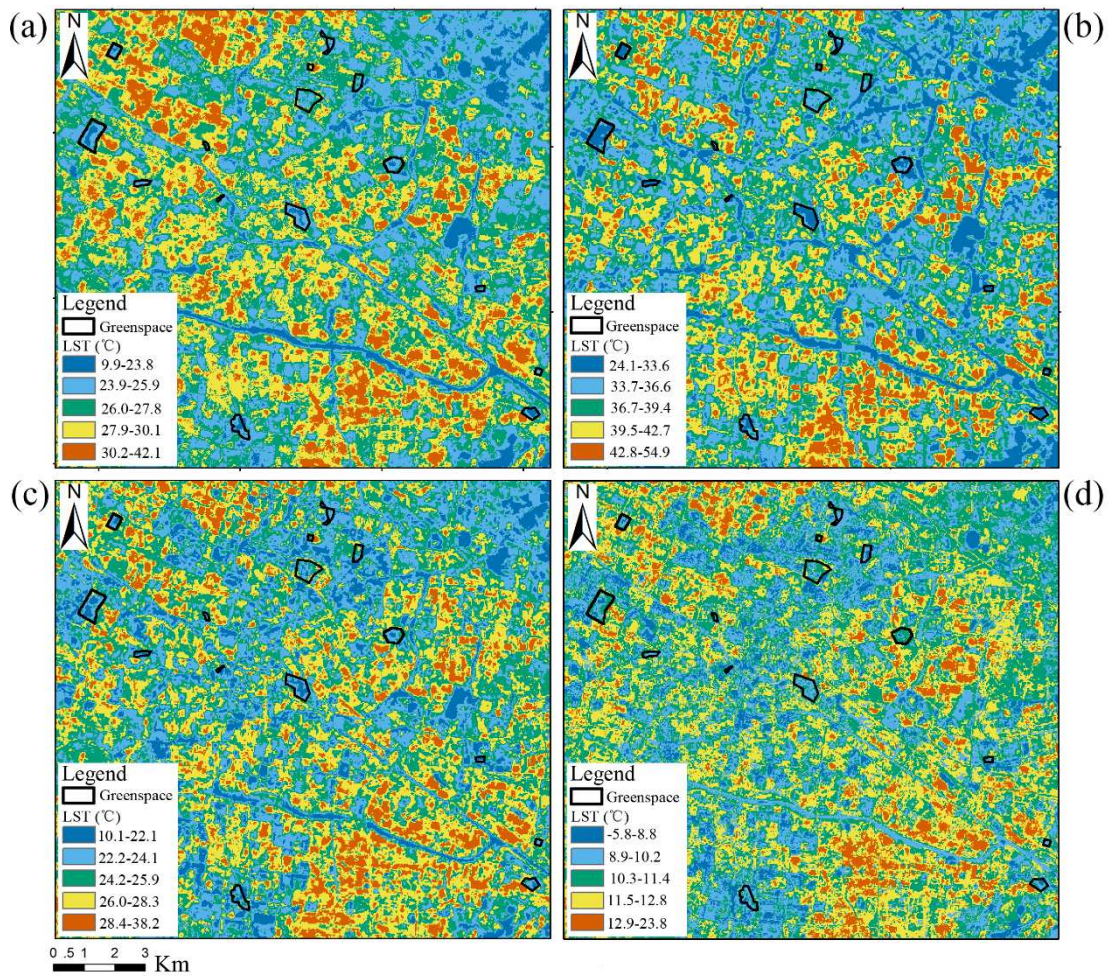
274 to identify aspects of tree diversity and community structure that had a significant
275 association with TDA or the cooling range (Schober et al., 2018). Then, variables that
276 had a significant association with cooling effects were included in multiple regression
277 models. Analyses were repeated for each season, all analyses were carried out in
278 SPSS 22.

279

280 **3. Results**

281 **3.1 The cooling effect of the greenspaces**

282 At the city scale, we found that the mean LST of the Changzhou central area was
283 $26.8 \pm 2.4^\circ\text{C}$, $37.7 \pm 3.7^\circ\text{C}$, $25.0 \pm 2.3^\circ\text{C}$, $11.1 \pm 1.3^\circ\text{C}$ in spring, summer, autumn and
284 winter respectively (Fig 2). Across the greenspaces, the mean LST was cooler
285 throughout the year, at $25.3 \pm 1.4^\circ\text{C}$, $34.2 \pm 2.4^\circ\text{C}$, $23.4 \pm 1.3^\circ\text{C}$, and $10.0 \pm 0.8^\circ\text{C}$
286 respectively. Most of the greenspaces had a lower LST than the surrounding area
287 throughout the year, except HH and CIT (greenspace abbreviations given in Figure 1
288 and Appendix 1). The temperature drop amplitude of HH was 0.0°C in spring, and the
289 temperature drop amplitude of CIT was 0.0°C in spring, summer, and autumn.

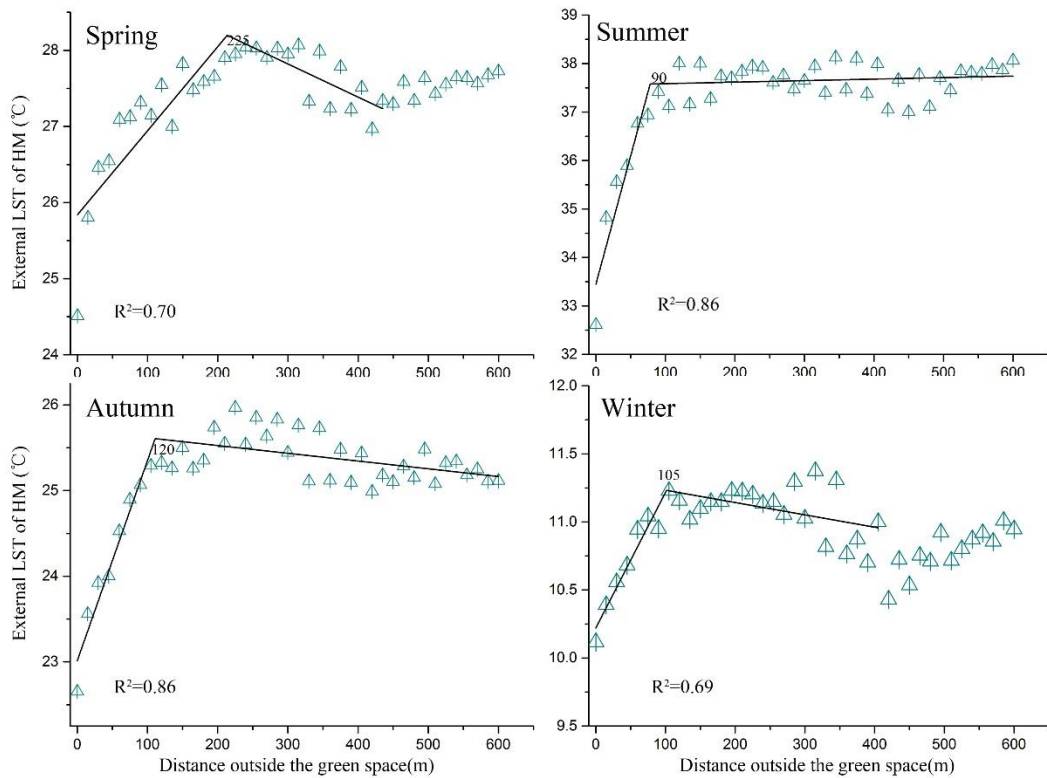


291 Figure 2 Land surface temperature for central Changzhou, China for (a) spring,
 292 (b) summer, (c) autumn and (d) winter. The 15 sampled greenspaces are outlined in
 293 black.

294 At the neighbourhood scale, piecewise regressions were used to determine the
 295 cooling range outside each greenspace (Figure 3, for greenspace HM as an example)
 296 in different seasons. The results show that the median cooling range across the 15
 297 greenspaces was 75 m (interquartile range (IQR) 45 m to 300 m), 75 m (IQR 30 m to
 298 255 m), 60 m (IQR 30 m to 120 m) and 60 m (IQR 30 m to 90 m) in spring, summer,
 299 autumn and winter respectively (Figure 4a). The median cooling range value of

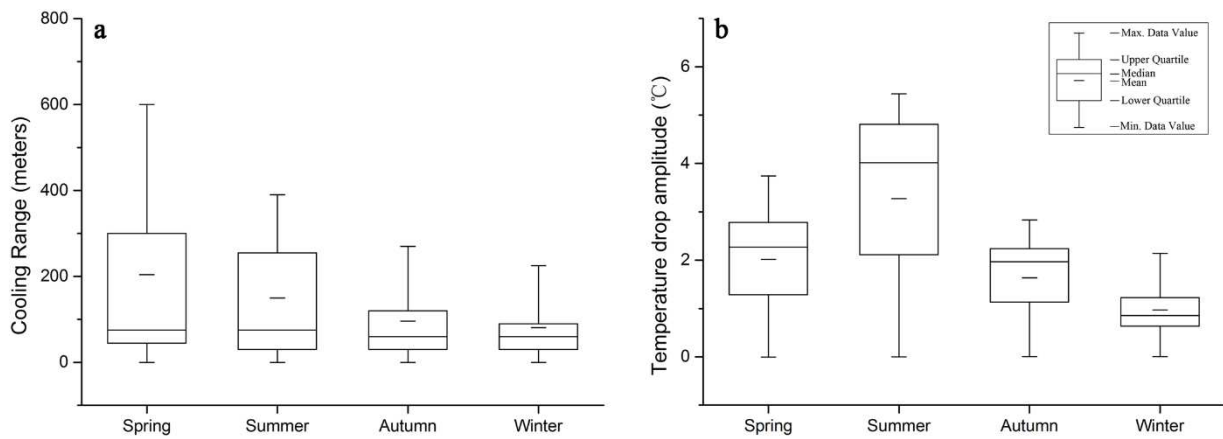
300 greenspaces was the same in spring and summer, and the same in autumn and winter,
 301 although they had different interquartile ranges. The cooling range of each greenspace
 302 varied across seasons, with the longest cooling ranges in spring, and the shortest in
 303 winter. For one of our greenspaces (CIT; Figure 1), the cooling range was near zero
 304 except in winter. Similarly XTD had no cooling range in winter. Greenspace XQ had
 305 the largest cooling range in spring and summer, while LS has the largest cooling range
 306 in autumn and winter (Table 1).

307



308

309 Figure 3 An example of cooling range and TDA for greenspaces “HM”. Across
 310 the four seasons, the cooling range was 225m, 90m, 120m and 105m, as estimated via
 311 the identification of turning points using piecewise analysis. TDA was 28.0°C-
 312 24.5°C=3.5°C, 37.4°C-32.6°C=4.8°C, 25.3°C-22.7°C=2.6°C, 11.2°C-10.1°C=1.1°C.



313 Figure 4 (a) The cooling range for 15 greenspaces in central Changzhou, China,
 314 across four seasons in 2017-2018. (b) The temperature drop amplitude of 15 green
 315 spaces across four seasons.

316

317 The TDA of each greenspace was calculated after the cooling range was
 318 determined by piecewise regression analysis. The TDA of greenspaces varied
 319 seasonally (Figure 4b); the median TDA of the 15 greenspaces was 2.3°C (IQR 1.3°C
 320 to 2.8°C), 4.0°C (IQR 2.1 to 4.8°C), 2.0°C (IQR 1.1°C to 2.2°C), and 0.9°C (IQR
 321 0.6°C to 1.2°C) in spring, summer, autumn and winter. The maximum TDA was,
 322 therefore, in summer and the minimum in winter. The TDA of each greenspace also
 323 varied seasonally (Table 1). The only exception to the general seasonal pattern was for
 324 greenspace CIT which had a near zero TDA in spring, summer and autumn, and a
 325 maximum, although still small, TDA in winter.

326

327 3.2 Plant community structure of the greenspaces

328 There was considerable variation in the number of trees present in each

329 greenspace. This was partly a consequence of the different proportion of green land,
330 water and impervious surface area in each greenspaces, and partly driven by the
331 history of the spaces. As Changzhou has urbanised, more greenspaces have been
332 constructed. The majority of these have been built within the last 20 years. Of those
333 we sampled, HM was the oldest. Built in 1960 it was redesigned in 2005. Given the
334 short history of greenspaces in the city, there are few mature trees. For instance, the
335 median DBH was 19.67 cm (IQR 17.30 cm to 21.54 cm), the 75% of trees have a
336 DBH smaller than 21.54 cm. This indicates that there are many young trees, as DBH
337 is a proxy of tree age. Similarly, median tree height was 7.1 m (IQR 6.9 m to 7.8 m),
338 and 25% of trees were between 7.8 m and 15 m tall. Around half of all trees were
339 shorter than 7.1 m. These trees can, therefore, act as a lower canopy layer and help to
340 form a more structured tree canopy, where taller trees are also present. Tree density
341 varied across the greenspaces. The median tree density was 235 trees/hectare (IQR
342 143 trees/hectare to 360 trees/hectare). The median crown height was 4.6 m (IQR 4.3
343 m to 4.7 m), the median crown width was 5.0 m (IQR 4.3 m to 5.7 m), and the median
344 tree canopy coverage was 52% (IQR 44% to 56%).

345 Of the 2082 trees that were sampled, 1253 (60.2%) were deciduous and the remainder
346 evergreen (Appendix 1). There were 49 deciduous tree species and 29 evergreen tree
347 species. The five most abundant deciduous tree species were *Acer palmatum* Thunb.
348 (195, 9.4%), *Metasequoia glyptostroboides* Hu et W. C. Cheng (140, 6.7%), *Cerasus*
349 *serrulata* (Lindl.) London var. *lannesiana* (Carri.) Makino (78, 3.8%), *Lagerstroemia*
350 *indica* Linn. (65, 3.1%), *Celtis sinensis* Pers. (63, 3%). The top five evergreen tree

351 species are *Cinnamomum camphora* (L.) Presl (223, 10.7%), *Osmanthus fragrans*
352 (Thunb.) Lour. (175, 8.4%), *Magnolia grandiflora* Linn. (83, 4%), *Trachycarpus*
353 *fortunei* (Hook.) H. Wendl. (59, 2.8%), *Photinia serrulata* Lindl. (46, 2.2%). The
354 median Shannon-Wiener diversity index was 2.48 (IQR 2.07 to 2.72), and the median
355 richness per plot was 1.92 (IQR 1.37 to 2.67).

356 Table 1. The cooling effect of 15 greenspaces within Changzhou city centre, China, across different seasons. Greenspace abbreviations are given
 357 in Figure 1 and Appendix 1.

Greenspace	Green land	TDA-spring	TDA-summer	TDA-autumn	TDA-winter	CR-Spring	CR-summer	CR-autumn	CR-winter
	Area (ha)	(°C)	(°C)	(°C)	(°C)	(m)	(m)	(m)	(m)
HD	1.03	0.65	2.05	1.13	1.12	75	60	45	90
HH	0.45	0.00	0.97	1.22	0.24	0	75	75	75
LS	2.12	2.61	3.07	2.20	1.23	255	225	270	225
HX	2.05	3.45	5.35	2.19	1.54	300	270	60	90
YX	2.76	2.27	3.49	1.66	0.64	75	30	75	15
WX	4.54	2.02	4.29	2.25	0.83	60	165	165	60
XQ	5.25	2.46	4.15	0.54	0.21	600	390	210	30
CIT	4.73	0.00	0.00	0.00	1.31	0	0	0	180
HE	6.10	2.78	4.99	2.83	2.14	30	30	30	60

WD	7.16	3.74	5.44	1.97	1.01	75	40	60	30
ZJ	12.76	1.28	2.49	2.02	0.85	180	15	15	60
XTD	12.10	2.21	4.42	0.74	0.00	390	375	45	0
HM	22.66	3.44	4.81	2.68	1.11	210	90	120	105
SM	19.54	1.31	2.11	1.42	0.64	45	45	30	15
QF	26.80	2.58	4.02	2.24	0.79	375	255	105	45

358

359 Table 2 Tree community structure of 15 greenspaces within Changzhou city centre, China.

Greenspace	Mean DBH (cm)	Mean height (m)	Density (trees/ha)	Mean crown height (m)	Mean crown width (m)	Tree canopy coverage (%)	Shannon-Wiener diversity index	Species richness per plot
HD	23.37	8.3	81.00	4.6	5.7	59.60	2.07	1.33
HH	19.67	7.1	15.00	3.4	3.3	13.80	1.27	1.00
LS	21.54	8.8	288.00	6.1	5.6	63.60	2.04	2.67
HX	18.88	6.9	231.00	4.7	5.9	56.30	2.40	2.50
YX	16.93	6.8	361.00	4.7	5.0	56.10	2.75	3.38
WX	21.25	7.2	235.00	4.2	5.9	54.20	2.51	2.13
XQ	20.27	7.1	219.00	4.6	5.7	52.30	2.24	1.87
CIT	19.67	7.1	48.00	3.4	3.0	29.30	1.52	1.37
HE	17.39	7.5	360.00	5.0	5.0	47.30	2.72	2.45

WD	12.22	6.8	418.00	3.5	3.5	54.20	3.01	2.80
ZJ	19.01	7.7	305.00	5.1	4.3	48.70	2.60	1.79
XTD	18.41	7.8	326.00	4.6	4.8	40.30	2.48	1.54
HM	26.46	9.2	143.00	6.9	5.5	60.20	2.67	1.92
SM	21.67	6.9	175.00	4.2	4.7	44.20	2.18	0.76
QF	16.31	6.1	678.00	3.8	4.5	45.40	3.24	3.19

360

361 **3.3 Associations between plant community structure and cooling effects**

362 There were no significant correlations between mean DBH, tree height, crown
363 height and the two measures of cooling effect across all seasons (Table 3a). However,
364 significant correlations were found for the remaining plant community structure
365 indicators and cooling effect. Firstly, in spring and summer, TDA was significantly
366 correlated with tree density, tree coverage, Shannon-Wiener diversity index, and
367 richness per plot. In autumn, TDA had a significant correlation with the Shannon-
368 Wiener diversity index and tree richness. However, plant community structure had no
369 significant correlation with TDA in winter. The correlation between CR and plant
370 community structure indicators differed from those with TDA. In spring, indicators
371 had no significant correlation with the CR, while in summer and autumn there was a
372 significant correlation for mean crown width, and in winter with tree density (Table
373 3a).

374 Table 3 For 15 greenspaces in central Changzhou, China the (a) correlation between cooling effect and plant community structure variables by
 375 seasons; and (b) correlation between variables. ** Significant at P<0.01, * Significant at P<0.05

376 (a)

Cooling effect	Seasons	Mean DBH	Mean Height	Density	Mean Crown Height	Mean Crown width	Tree- coverage	Shannon-Wiener diversity index	Richness per plot
Temperature drop amplitude	Spring	-0.246	-0.063	0.583*	0.454	0.438	0.653**	0.754**	0.681**
	Summer	-0.267	-0.02	0.569*	0.358	0.505	0.581*	0.772**	0.598*
	Autumn	-0.016	0.104	0.447	0.5	0.371	0.485	0.598*	0.534*
	Winter	-0.003	0.232	0.048	0.261	0.131	0.328	0.154	0.292
Cooling range	Spring	-0.095	0.145	0.368	0.435	0.425	0.344	0.274	0.359
	Summer	0.125	0.131	0.03	0.118	0.556*	0.159	-0.07	0.113
	Autumn	0.191	0.092	0.09	0.172	0.543*	0.487	0.075	0.448
	Winter	0.473	0.469	-0.518*	0.188	0.11	0.348	-0.455	-0.072

377 (b)

Variables	Height	Density	Crown height	Crown width	Tree- coverage	Shannon-Wiener diversity index	Richness per plot
Mean DBH	0.624*	-0.627*	0.587*	0.471	0.182	-0.406	-0.514
Mean height		-0.341	0.578*	0.331	0.358	-0.316	-0.318
Density			-0.022	0.06	0.296	0.851**	0.764**
Mean crown height				0.619*	0.639*	0.218	0.158
Mean crown width					0.745**	0.271	0.215
Tree coverage						0.558*	0.507
Shannon-Wiener diversity index							0.704**

378

379 To quantify the relationship between cooling effect variables and plant
380 community structure we carried out multiple regressions using those community
381 structure variables that had significant correlations with the cooling effect as predictor
382 variables. However, many of the plant community structure variables were also
383 significantly inter-correlated (Table 3b). To avoid violating assumptions of multiple
384 regression we therefore used the Shannon-Wiener diversity index (represented by ‘H’
385 in equation 6 to 16) and tree coverage (% , represented by ‘T’) only in our regression
386 models. We selected the models from Table 4 with the highest adjusted R² value for
387 the final model of TDA and CR in different seasons. Equations 6 to 8 describe the
388 TDA prediction models for greenspaces community structure in spring, summer and
389 autumn.

390 Table 4. Parameter estimates for the relationship between TDA and plant community
391 structure across different seasons.

	Shannon-Wiener diversity index	Tree coverage	Intercept	Adjusted R ²	p
TDA Spring	1.29	3.07	-2.49	0.59	0.002
TDA Summer	2.03	2.74	-2.72	0.57	0.003
TDA Autumn	0.93		-0.55	0.31	0.018

392 $TDA_{Spring} = - 2.49 + 3.07T + 1.29H \quad (R^2 = 0.59, P=0.002) \quad (6)$

393 $TDA_{Summer} = - 2.72 + 2.74T + 2.03H \quad (R^2 = 0.57, P=0.003) \quad (7)$

394 $TDA_{Autumn} = - 0.55 + 0.93H \quad (R^2 = 0.31, P=0.018) \quad (8)$

395 For TDA, in spring, our regression model (Equation 6) explained 59% of the

396 variation. With the Shannon-Wiener diversity index kept constant, TDA increases
 397 0.31°C for every 10% increase in tree coverage. When tree coverage is kept constant,
 398 TDA increases by 0.13°C for every 0.1 increase in the Shannon-Wiener diversity
 399 index. In summer, our model (Equation 7) explained 57% of the variance. When the
 400 Shannon-Wiener diversity index is kept constant, TDA increases by 0.27°C for every
 401 10% increase in tree coverage. When the tree coverage is kept constant, TDA
 402 increases 0.2°C for every 0.1 increase in Shannon-Wiener diversity index. In autumn,
 403 our model (Equation 8) explained 31% of the variance and TDA amplitude increases
 404 0.09°C for every 0.1 increase in Shannon Wiener diversity index.

$$405 \quad \text{CR Summer} = -178.4 + 65.4W \quad (R^2=0.15, P=0.082) \quad (9)$$

$$406 \quad \text{CR Autumn} = -114.8 + 41.8W \quad (R^2=0.21, P=0.048) \quad (10)$$

$$407 \quad \text{CR Winter} = -0.13D + 105.5 \quad (R^2=0.06, P=0.201) \quad (11)$$

408 In summer, autumn and winter, the cooling range (CR) is significantly correlated
 409 with both the mean crown width and tree density; we therefore included mean crown
 410 width in metres ('W' in Equations 9 and 10), and density (trees/hectare, represented as
 411 'D' in Equations 11) in our regression models. In summer, our regression model
 412 (Equation 9) explained 15% of the variation. Cooling range increases 65.4 metres for
 413 every 1-metre increase in mean crown width. In autumn, our model (Equation 10)
 414 explains 21% of the variation. The cooling range increases by 41.8 metres for every 1-
 415 metre increase in mean crown width. In winter, our model (Equation 11) explains 6%
 416 of the variance and the cooling range decreases by 1.3 metres for every 10 trees per
 417 hectare increase.

418

419 **4. Discussion**

420 **4.1 Influence of tree diversity on cooling effect**

421 Biodiversity underpins the delivery of ecosystem function (Cardinale et al.,
422 2011), and, therefore many ecosystem services. Indeed, tree species richness of forests
423 shows a positive relationship with the provision of multiple ecosystem services
424 (Gamfeldt et al., 2013). Despite this, to date, most research on the extent to which
425 urban greenspaces might mitigate urban heat island effects has concentrated on
426 quantifying the threshold size of greenspaces (Fan et al., 2019; Yu et al., 2020),
427 greenspace configuration (Du et al., 2017; Lin et al., 2015), and particular structural
428 characteristics such as canopy coverage (Giridharan et al., 2008; Petri et al., 2019;
429 Yang et al., 2017) or tree height (Zhang et al., 2013), rather than exploring the role of
430 tree diversity *per se*. Here we show that when the tree coverage keep constant the
431 diversity of the tree community within greenspaces can have a significant effect on
432 the magnitude of cooling effect in spring, summer and autumn, and maximum TDA
433 benefit in summer. If cities, and their residents, are to make best use of greenspaces as
434 one way to mitigate urban heat island effects, then ensuring that tree diversity is taken
435 into account should be a central consideration.

436

437 There are substantial differences between tree species in terms of their ability to
438 cool the surrounding air (Bau-Show and Yann-Jou, 2010; Rahman et al., 2015). Tree
439 canopies with high leaf area and transpiration rates have been shown to be the most

440 effective in terms of cooling (Rahman et al., 2018). Canopy shape and leaf colour of
441 tree species may influence their cooling efficiency (Feyisa et al., 2014). Further, a
442 plant community with multiple layers of trees, shrubs and herbs can decrease air
443 temperature by 1°C on a sunny day, and 0.5 °C on a cloudy day in summer, compared
444 with a simple biomass structure dominated by a tall canopy layer (Fung and Jim,
445 2019). A combination of tree species with high cooling efficiencies could improve the
446 magnitude of cooling effects provided by greenspaces. Where space is limited, such a
447 diversity of trees are likely to be more efficient at intercepting solar radiation before it
448 reaches the surface, and also in providing a greater leaf area to enhance transpiration
449 rates, further ameliorating cooling effects. Further, such a community structure is
450 likely to result in greater levels of biomass production (Gamfeldt et al., 2013), which
451 will, over time, increase the effectiveness of cooling, as larger and larger leaf surface
452 areas will be produced.

453 **4.2 Plant community structure and variation in cooling effects across seasons**

454 Our work was carried out in a sub-tropical location, characterised by seasons
455 delineated by changes in air temperature and solar radiation, we would therefore
456 expect the cooling effects of greenspaces to vary seasonally. In line with our
457 expectations, we find that the cooling effects are greatest in summer and least in
458 winter (Jenerette et al., 2011; Mingjuan et al., 2019). Although we find some
459 differences in terms of the magnitude of cooling effects in spring and autumn, our
460 findings also align with research in Shenzheng, China, where the TDA of parks was
461 greatest in in summer (4.6°C), followed by autumn (4.0°C) and spring (3.8°C), TDA

462 was least in winter (2.9°C) (Zhang et al., 2013). Given the role that tree species
463 diversity plays in explaining cooling effects, the cooling effect efficacy of the main
464 species found in those cities, as well as climatic and seasonality variations, could
465 explain the differences between the two studies.

466

467 We found that the importance of tree species diversity in explaining cooling
468 effects varies seasonally. This might be due to the fact that the dominant tree species,
469 which each constitute over 4% of the sampled tree numbers, namely *Acer palmatum*,
470 *Metasequoia glyptostroboides*, *Cinnamomum camphora*, *Osmanthus fragrans*,
471 *Magnolia grandiflora*., exhibit changes in transpiration rates between seasons, from
472 very high levels to in summer to very weak in winter (Mingjuan et al., 2019; Peters et
473 al., 2010). Shading efficiency is also associated with the seasonal variation of leaf
474 cover, resulting in deciduous tree species having very low shading function in winter,
475 while evergreen tree species can provide shade throughout the year. Therefore, the
476 cooling effect of a plant community is consistent with how the seasonal climate
477 changes alters vegetation physiology, as well as the specific characteristics of
478 individual tree species.

479 The picture for the cooling range of our greenspaces was more complex. There
480 are two sets of factors that will influence the cooling range of a greenspace, one is the
481 characteristics of the greenspace itself such as the size (Zhang et al., 2009) and shape
482 (Du et al., 2017; Lin et al., 2015). The second set of factors relate to the nature of the
483 built up area surrounding the greenspace (Lin et al., 2015; Shiflett et al., 2017). In

484 cities, heat is stored and re-radiated from massive and complex urban structures
485 (Rizwan Ahmed Memon et al., 2008) and these heat sources outside the greenspaces
486 bring uncertainty to the prediction of the cooling range, such as the uneven
487 distribution of buildings and the heat released from air conditioner units in the
488 summer. We found that the mean crown width and tree density of the greenspace can
489 explain part of the variation in the cooling range. In terms of plant community
490 structure, trees with the widest crowns will generate more shading and potentially
491 more evapotranspiration in summer and autumn. However, the explanatory power of
492 our models for the cooling range was substantially lower than those for temperature
493 drop amplitude. CIT is an exception amongst the greenspaces in our study as it
494 provides no cooling to the surrounding area in spring, summer and autumn. There are
495 a number of possible reasons for this. Firstly, there are greater number of impervious
496 surfaces in CIT than other greenspaces. Additionally, the green land that is present has
497 some of the lowest tree coverage, tree density and tree diversity values of all the
498 greenspaces we studied. It is also possible that the urban area surrounding CIT has a
499 better cooling potential than the CIT greenspace itself; specifically there is a river to
500 the east of CIT. Whilst previous research indicates that tree height may also influence
501 temperature reduction (Zhang et al., 2013), We do not find a significant relationship
502 between the mean tree height of a greenspace and its cooling effect (also see (Speak et
503 al., 2020). This emphasizes the greater complexity involved in understanding how
504 cooling effects from greenspaces propagate into the built-up areas that surround them.
505

506

507 More generally, urban greenspaces are composed of trees, shrubs, and
508 grassland, and the components play a different cooling function in different seasons
509 (Feyisa et al., 2014; Oliveira and Costa, 2012; Yu et al., 2020). Trees act as heat-sinks
510 in all seasons, grassland serves as a heat-sink only in summer and spring-autumn, but
511 it become a heat-source in winter as the increased amount of bare soil can change the
512 thermal characteristics of this vegetation type (Yu et al., 2020). Trees maintain greater
513 physiological activity in warm seasons with sufficient water to support them (Oliveira
514 and Costa, 2012). More solar radiation energy can reach the ground surface and lower
515 layers of greenspaces in winter after leaves fall from deciduous trees (Wang et al.,
516 2016). The increasing solar radiation and weak shading and transpiration of plant
517 community decreases the total cooling effect of greenspaces in winter, and may
518 explain the negative correlation between tree density and cooling range. Despite this
519 seasonal variation, enhancing tree diversity within greenspaces remains an important
520 UHIE mitigation tool as cooling effects will be more beneficial to a city and its
521 residents in warmer, summer months, rather than cooler, winter months.

522

523 **4.3 Conclusions and implications for future study and greenspace design**

524 Urban greenspace planning needs to accommodate a wide range of conflicting
525 demands on space and resources (Littke, 2015). If urban planners wish to make the
526 most use of greenspaces as an UHIE mitigation tool, it will be increasingly important
527 to optimise tree community structure within those greenspaces. Shannon-Wiener

528 diversity index can, therefore, be used as an indicator of the likely cooling effect of
529 tree stands, woodlands and forests as this metric is positively associated with cooling
530 effects in spring, summer and autumn. Given the importance of tree diversity for the
531 delivery of several other ecosystem services (McCarthy et al., 2011), taking such an
532 approach, rather than planting stands of single/few species, is also likely to deliver
533 other benefits for city residents.

534 Despite the benefits that diverse tree communities can deliver, it is common that
535 one or several tree species become dominant in urban greenspaces (Nagendra and
536 Gopal, 2011). We also found the tree species are not distributed evenly in
537 Changzhou's greenspaces, with a few species, such as *Cinnamomum camphora*, *Acer*
538 *palmatum*, and *Osmanthus fragrans*, being substantially more abundant than others.
539 Ensuring that a handful of species do not become dominant is one way that urban
540 planners can raise the Shannon-Wiener diversity index, which takes into account
541 species evenness as well as richness (Strong, 2016). For new greenspaces, landscape
542 designers and city planners could, therefore, include a greater diversity of species, and
543 plant those species evenly if they wish to maximise the Shannon-Wiener diversity
544 index, and the resulting cooling effects. For the existing greenspaces, it may take
545 longer to diversify the tree community structure. This could be done, however, by
546 ensuring that a broader range of tree species are considered when replacing dead or
547 diseased trees.

548 In addition to diversity, we recommend that canopy coverage, canopy width, and
549 density are all prioritised when it comes to designing greenspaces to maximise their

550 role in mitigating the UHIE. Increasing tree canopy coverage results in a greater
551 cooling effect, as does ensuring that tree crowns are wide (Zhou et al., 2014; Ziter et
552 al., 2019), something that is associated with higher light attenuation and, therefore a
553 greater cooling effect (Speak et al., 2020). In contrast, we do not find a significant
554 relationship between the mean DBH, tree height, and crown height of greenspace and
555 its cooling effect, so these indicators should not be prioritised.

556 Our findings are based on observational data so are correlational only. Future
557 research should be undertaken using more rigorous designs, such as ‘before-after-
558 control-intervention (BACI)’ which would enable cooling effects to be more directly
559 attributed to tree community composition metrics that we have identified here. Further
560 potential research topics include: (1) identify how transpiration and shading efficiency
561 varies between tree species. Here we found that tree diversity could enhance the
562 cooling effect of plant community. It is likely that the cooling benefit could be further
563 enhanced if the tree community was also composed of a mix of species that are known
564 to be particularly efficient in providing shade and/or transpiration. However, we still
565 know relatively little about these particular characteristics and how they might result
566 in increased cooling potential (Rahman et al., 2015; Stratópoulos et al., 2018). What
567 we do know, suggests that substantial improvements could be made. For instance in
568 Manchester, UK *Pyrus calleryana* and *Crataegus laevigata* provided 3 to 4 times
569 greater cooling than *Prunus ‘Umineko’*, *Sorbus arnoldiana* or *Malus ‘Rudolph’*
570 (Rahman et al., 2015).(2) The mechanism that underpins how tree diversity underpins
571 any cooling effect is still unclear. Further studies, including those of a more

572 experimental nature, are required to explore and understand these mechanisms.

573

574

575 **Declaration of Competing Interest**

576 The authors declare that they have no known competing financial interests or
577 personal relationships that could have appeared to influence the work reported in this
578 paper.

579 **CRedit Author Statement**

580 **Xinjun Wang:** Methodology, Investigation, Writing- Original draft preparation.

581 **Martin Dallimer:** Formal analysis, Writing- Reviewing and Editing. **Catherine E.**

582 **Scott:** Formal analysis, Writing- Reviewing and Editing. **Weiting Shi:** Investigation.

583 **Jixi Gao:** Conceptualization.

584 **Acknowledgments**

585 The research was supported by the National Key Research and Development
586 Plan of China [No.2017YFC0506606], the Natural Environment Research Council
587 [grant NE/S015396/1], the Postdoctoral Research Funding of Jiangsu [grant
588 2019K270], Changzhou Landscape Technology Project [grant 19-20JH13], and
589 Jiangsu Overseas Visiting Scholar Program for University prominent Young &
590 Middle-aged Teachers and Presidents. The authors would like to express the sincere
591 thanks to volunteers for helping collect field data from the sample plots.

592

593 **References**

- 594 Argüeso D, Evans JP, Pitman AJ, Di Luca A. Effects of city expansion on heat stress under climate change
595 conditions. *PloS one* 2015; 10: e0117066-e0117066.
- 596 Bau-Show L, Yann-Jou L. Cooling Effect of Shade Trees with Different Characteristics in a Subtropical
597 Urban Park. *HortScience horts* 2010; 45: 83-86.
- 598 Bernatzky A. The contribution of trees and green spaces to a town climate. *Energy and Buildings* 1982;
599 5: 1-10.
- 600 Boumans RJM, Phillips DL, Victory W, Fontaine TD. Developing a model for effects of climate change on
601 human health and health–environment interactions: Heat stress in Austin, Texas. *Urban
602 Climate* 2014; 8: 78-99.
- 603 Bowler DE, Buyung-Ali L, Knight TM, Pullin AS. Urban greening to cool towns and cities: A systematic
604 review of the empirical evidence. *Landscape and Urban Planning* 2010; 97: 147-155.
- 605 Buyantuyev A, Wu J. Urban heat islands and landscape heterogeneity: linking spatiotemporal variations
606 in surface temperatures to land-cover and socioeconomic patterns. *Landscape Ecology* 2010;
607 25: 17-33.
- 608 Cao X, Onishi A, Chen J, Imura H. Quantifying the cool island intensity of urban parks using ASTER and
609 IKONOS data. *Landscape and Urban Planning* 2010; 96: 224-231.
- 610 Cardinale BJ, Matulich KL, Hooper DU, Byrnes JE, Duffy E, Gamfeldt L, et al. The functional role of
611 producer diversity in ecosystems. *American Journal of Botany* 2011; 98: 572-592.
- 612 Chang C-R, Li M-H. Effects of urban parks on the local urban thermal environment. *Urban Forestry &
613 Urban Greening* 2014; 13: 672-681.
- 614 Changzhou Statistics Bureau. National Economic and Social Development Statistics Bulletin of
615 Changzhou of 2018. 2019, 2019.
- 616 Chen G, Singh KK, Lopez J, Zhou Y. Tree canopy cover and carbon density are different proxy indicators
617 for assessing the relationship between forest structure and urban socio-ecological conditions.
618 *Ecological Indicators* 2020; 113: 106279.
- 619 Dimoudi A, Nikolopoulou M. Vegetation in the urban environment: microclimatic analysis and benefits.
620 *Energy and Buildings* 2003; 35: 69-76.
- 621 Du H, Cai W, Xu Y, Wang Z, Wang Y, Cai Y. Quantifying the cool island effects of urban green spaces using
622 remote sensing Data. *Urban Forestry & Urban Greening* 2017; 27: 24-31.
- 623 Fan H, Yu Z, Yang G, Liu TY, Liu TY, Hung CH, et al. How to cool hot-humid (Asian) cities with urban trees?
624 An optimal landscape size perspective. *Agricultural and Forest Meteorology* 2019; 265: 338-
625 348.
- 626 Feyisa GL, Dons K, Meilby H. Efficiency of parks in mitigating urban heat island effect: An example from
627 Addis Ababa. *Landscape and Urban Planning* 2014; 123: 87-95.
- 628 Fu H, Chen J. Formation, features and controlling strategies of severe haze-fog pollutions in China.
629 *Science of The Total Environment* 2017; 578: 121-138.
- 630 Fung CKW, Jim CY. Microclimatic resilience of subtropical woodlands and urban-forest benefits. *Urban
631 Forestry & Urban Greening* 2019; 42: 100-112.
- 632 Gamfeldt L, Snäll T, Bagchi R, Jonsson M, Gustafsson L, Kjellander P, et al. Higher levels of multiple
633 ecosystem services are found in forests with more tree species. *Nature Communications* 2013;
634 4: 1340.
- 635 Giridharan R, Lau SSY, Ganesan S, Givoni B. Lowering the outdoor temperature in high-rise high-density

636 residential developments of coastal Hong Kong: The vegetation influence. *Building and*
637 *Environment* 2008; 43: 1583-1595.

638 Grilo F, Pinho P, Aleixo C, Catita C, Silva P, Lopes N, et al. Using green to cool the grey: Modelling the
639 cooling effect of green spaces with a high spatial resolution. *Science of The Total Environment*
640 2020; 724: 138182.

641 Guhathakurta S, Gober P. The Impact of the Phoenix Urban Heat Island on Residential Water Use. *Journal*
642 *of the American Planning Association* 2007; 73: 317-329.

643 Haashemi S, Weng Q, Darvishi A, Alavipanah KS. Seasonal Variations of the Surface Urban Heat Island
644 in a Semi-Arid City. *Remote Sensing* 2016; 8.

645 Hardin PJ, Jensen RR. The effect of urban leaf area on summertime urban surface kinetic temperatures:
646 A Terre Haute case study. *Urban Forestry & Urban Greening* 2007; 6: 63-72.

647 i-Tree. *i-Tree Manuals & Workbooks*. 2020, 2020.

648 i-Tree Canopy. *i-Tree Canopy manual & workspace*. 2020, 2020.

649 IPCC. *Impacts of 1.5°C of Global Warming on Natural and Human Systems*. 2020, 2018.

650 Jenerette GD, Harlan SL, Stefanov WL, Martin CA. Ecosystem services and urban heat riskscape
651 moderation: water, green spaces, and social inequality in Phoenix, USA. *Ecological Applications*
652 2011; 21: 2637-2651.

653 Jim CY. Impacts of intensive urbanization on trees in Hong Kong. *Environmental Conservation* 1998; 25:
654 146-159.

655 Jonsson P. Vegetation as an urban climate control in the subtropical city of Gaborone, Botswana.
656 *International Journal of Climatology* 2004; 24: 1037-1322.

657 Kelliher FM, Leuning R, Schulze ED. Evaporation and canopy characteristics of coniferous forests and
658 grasslands. *Oecologia* 1993; 95: 153-163.

659 Leuzinger S, Vogt R, Körner C. Tree surface temperature in an urban environment. *Agricultural and Forest*
660 *Meteorology* 2010; 150: 56-62.

661 Li J, Song C, Cao L, Zhu F, Meng X, Wu J. Impacts of landscape structure on surface urban heat islands: A
662 case study of Shanghai, China. *Remote Sensing of Environment* 2011; 115: 3249-3263.

663 Lin W, Yu T, Chang X, Wu W, Zhang Y. Calculating cooling extents of green parks using remote sensing:
664 Method and test. *Landscape and Urban Planning* 2015; 134: 66-75.

665 Littke H. Planning the Green Walkable City: Conceptualizing Values and Conflicts for Urban Green Space
666 Strategies in Stockholm. *Sustainability* 2015; 7: 11306-11320.

667 Liu W, You H, Dou J. Urban-rural humidity and temperature differences in the Beijing area. *Theoretical*
668 *and Applied Climatology* 2009; 96: 201-207.

669 Loreau M, Naeem S, Inchausti P, Bengtsson J, Grime JP, Hector A, et al. Biodiversity and Ecosystem
670 Functioning: Current Knowledge and Future Challenges. *Science* 2001; 294: 804.

671 Lu J, Li Q, Zeng L, Chen J, Liu G, Li Y, et al. A micro-climatic study on cooling effect of an urban park in a
672 hot and humid climate. *Sustainable Cities and Society* 2017; 32: 513-522.

673 Luber G, McGeehin M. Climate Change and Extreme Heat Events. *American Journal of Preventive*
674 *Medicine* 2008; 35: 429-435.

675 Martin NA, Chappelka AH, Somers G, Loewenstein EF, Keever GJ. Evaluation of Sampling Protocol for i-
676 Tree Eco: A Case Study in Predicting Ecosystem Services at Auburn University. *Arboriculture &*
677 *Urban Forestry* 2013; 39: 56-61.

678 Masoudi M, Tan PY. Multi-year comparison of the effects of spatial pattern of urban green spaces on
679 urban land surface temperature. *Landscape and Urban Planning* 2019; 184: 44-58.

680 McCarthy HR, Pataki DE, Jenerette GD. Plant water-use efficiency as a metric of urban ecosystem
681 services. *Ecological Applications* 2011; 21: 3115-3127.

682 McDonald RI, Green P, Balk D, Fekete BM, Revenga C, Todd M, et al. Urban growth, climate change, and
683 freshwater availability. *Proceedings of the National Academy of Sciences* 2011; 108: 6312.

684 Mingjuan Z, Xiao W, Xiaolei S, Chen L, Peifan L. Microclimate regulating effects of plant communities
685 with different structures in summer and winter in Nanjing City. *Chinese Journal of Ecology* 2019;
686 38: 27-34.

687 Morris KI, Chan A, Morris KJK, Ooi MCG, Oozeer MY, Abakr YA, et al. Impact of urbanization level on the
688 interactions of urban area, the urban climate, and human thermal comfort. *Applied Geography*
689 2017; 79: 50-72.

690 Moser A, Rötzer T, Pauleit S, Pretzsch H. Structure and ecosystem services of small-leaved lime (*Tilia*
691 *cordata* Mill.) and black locust (*Robinia pseudoacacia* L.) in urban environments. *Urban Forestry*
692 *& Urban Greening* 2015; 14: 1110-1121.

693 Moss JL, Doick KJ, Smith S, Shahrestani M. Influence of evaporative cooling by urban forests on cooling
694 demand in cities. *Urban Forestry & Urban Greening* 2019; 37: 65-73.

695 Nagendra H, Gopal D. Tree diversity, distribution, history and change in urban parks: studies in Bangalore,
696 India. *Urban Ecosystems* 2011; 14: 211-223.

697 Nowak DJ, Crane, Daniel E., Stevens, Jack C., Hoehn, Robert E., Walton, Jeffrey T. A ground-based
698 method of assessing urban forest structure and ecosystem services. *Arboriculture & Urban*
699 *Forestry* 2008; 34: 347-358.

700 Oke TR. City size and the urban heat island. *Atmospheric Environment (1967)* 1973; 7: 769-779.

701 Oliveira G, Costa A. How resilient is *Quercus suber* L. to cork harvesting? A review and identification of
702 knowledge gaps. *Forest Ecology and Management* 2012; 270: 257-272.

703 Perini K, Magliocco A. Effects of vegetation, urban density, building height, and atmospheric conditions
704 on local temperatures and thermal comfort. *Urban Forestry & Urban Greening* 2014; 13: 495-
705 506.

706 Peters EB, McFadden JP, Montgomery RA. Biological and environmental controls on tree transpiration
707 in a suburban landscape. *Journal of Geophysical Research: Biogeosciences* 2010; 115.

708 Petri AC, Wilson B, Koeser A. Planning the urban forest: Adding microclimate simulation to the planner's
709 toolkit. *Land Use Policy* 2019; 88: 104117.

710 Qin D, Yan H, Zhengcui L, Tianjiao M, Hua C, Jie X. The characteristic of climate warming and its impact
711 on the severe climate. *Climate Change Branch of Chinese Meteorological Society 2008 Annual*
712 *Meeting, Beijing, China, 2008*, pp. 10.

713 Qin Z-h, Li W-j, Xu B, Zhang W-c. The estimation of land surface emissivity for LANDSAT TM6. *Remote*
714 *Sensing for Land & Resources* 2004; 3: 28-36.

715 Qiu K, Jia B. The roles of landscape both inside the park and the surroundings in park cooling effect.
716 *Sustainable Cities and Society* 2020; 52: 101864.

717 Rahman MA, Armson D, Ennos AR. A comparison of the growth and cooling effectiveness of five
718 commonly planted urban tree species. *Urban Ecosystems* 2015; 18: 371-389.

719 Rahman MA, Moser A, Gold A, Rötzer T, Pauleit S. Vertical air temperature gradients under the shade of
720 two contrasting urban tree species during different types of summer days. *Science of The Total*
721 *Environment* 2018; 633: 100-111.

722 Ren Y, Deng L-Y, Zuo S-D, Song X-D, Liao Y-L, Xu C-D, et al. Quantifying the influences of various ecological
723 factors on land surface temperature of urban forests. *Environmental Pollution* 2016; 216: 519-

724 529.

725 Richards DR, Fung TK, Belcher RN, Edwards PJ. Differential air temperature cooling performance of
726 urban vegetation types in the tropics. *Urban Forestry & Urban Greening* 2020; 50: 126651.

727 Rizwan Ahmed Memon, Dennis Y. C. Leung, Chunho L. A review on the generation, determination and
728 mitigation of urban heat island. *Journal of environmental sciences* 2008; 201: 120-128.

729 Salvati A, Coch Roura H, Cecere C. Assessing the urban heat island and its energy impact on residential
730 buildings in Mediterranean climate: Barcelona case study. *Energy and Buildings* 2017; 146: 38-
731 54.

732 Santamouris M. Recent progress on urban overheating and heat island research. Integrated assessment
733 of the energy, environmental, vulnerability and health impact. Synergies with the global
734 climate change. *Energy and Buildings* 2020; 207: 109482.

735 Schober P, Boer C, Schwarte LA. Correlation Coefficients: Appropriate Use and Interpretation.
736 *Anesthesia & Analgesia* 2018; 126.

737 Seto KC, Güneralp B, Hutyrá LR. Global forecasts of urban expansion to 2030 and direct impacts on
738 biodiversity and carbon pools. *Proceedings of the National Academy of Sciences* 2012; 109:
739 16083-16088.

740 Shahidan MF, Shariff MKM, Jones P, Salleh E, Abdullah AM. A comparison of *Mesua ferrea* L. and *Hura*
741 *crepitans* L. for shade creation and radiation modification in improving thermal comfort.
742 *Landscape and Urban Planning* 2010; 97: 168-181.

743 Shekhar S, Aryal J. Role of geospatial technology in understanding urban green space of Kalaburagi city
744 for sustainable planning. *Urban Forestry & Urban Greening* 2019; 46: 126450.

745 Shi Y-r, Zhang Y-f. Remote sensing retrieval of urban land surface temperature in hot-humid region.
746 *Urban Climate* 2018; 24: 299-310.

747 Shiflett SA, Liang LL, Crum SM, Feyisa GL, Wang J, Jenerette GD. Variation in the urban vegetation,
748 surface temperature, air temperature nexus. *Science of The Total Environment* 2017; 579: 495-
749 505.

750 Speak A, Montagnani L, Wellstein C, Zerbe S. The influence of tree traits on urban ground surface shade
751 cooling. *Landscape and Urban Planning* 2020; 197: 103748.

752 Srivanit M, Hokao K. Evaluating the cooling effects of greening for improving the outdoor thermal
753 environment at an institutional campus in the summer. *Building and Environment* 2013; 66:
754 158-172.

755 Stratópoulos LMF, Duthweiler S, Häberle K-H, Pauleit S. Effect of native habitat on the cooling ability of
756 six nursery-grown tree species and cultivars for future roadside plantings. *Urban Forestry &*
757 *Urban Greening* 2018; 30: 37-45.

758 Strong WL. Biased richness and evenness relationships within Shannon–Wiener index values. *Ecological*
759 *Indicators* 2016; 67: 703-713.

760 Sun R, Chen A, Chen L, Lü Y. Cooling effects of wetlands in an urban region: The case of Beijing. *Ecological*
761 *Indicators* 2012; 20: 57-64.

762 Tang Z, Ren Z-b, Zhang H-f, He X-y. Cooling effects of urban forest community structure. *Chinese Journal*
763 *of Applied Ecology* 2017; 28: 2823-2830.

764 United Nations. 2014 revision of the World Urbanization Prospects. 2020, 2014.

765 Vaz Monteiro M, Doick KJ, Handley P, Peace A. The impact of greenspace size on the extent of local
766 nocturnal air temperature cooling in London. *Urban Forestry & Urban Greening* 2016; 16: 160-
767 169.

768 Verdú-Vázquez A, Fernández-Pablos E, Lozano-Diez RV, López-Zaldívar Ó. Development of a
769 methodology for the characterization of urban and periurban green spaces in the context of
770 supra-municipal sustainability strategies. *Land Use Policy* 2017; 69: 75-84.

771 Wang M, Chang H-C, Merrick JR, Amati M. Assessment of solar radiation reduction from urban forests
772 on buildings along highway corridors in Sydney. *Urban Forestry & Urban Greening* 2016; 15:
773 225-235.

774 Wang X-j, Cheng H-m, Xi J, Yang G-y, Zhao Y-w. Relationship between Park Composition, Vegetation
775 Characteristics and Cool Island Effect. *Sustainability* 2018; 10: 587.

776 Wolch JR, Byrne J, Newell JP. Urban green space, public health, and environmental justice: The challenge
777 of making cities 'just green enough'. *Landscape and Urban Planning* 2014; 125: 234-244.

778 Yang A-S, Juan Y-H, Wen C-Y, Chang C-J. Numerical simulation of cooling effect of vegetation
779 enhancement in a subtropical urban park. *Applied Energy* 2017; 192: 178-200.

780 Yang G, Yu Z, Jørgensen G, Vejre H. How can urban blue-green space be planned for climate adaption in
781 high-latitude cities? A seasonal perspective. *Sustainable Cities and Society* 2020a; 53: 101932.

782 Yang X, Peng LLH, Jiang Z, Chen Y, Yao L, He Y, et al. Impact of urban heat island on energy demand in
783 buildings: Local climate zones in Nanjing. *Applied Energy* 2020b; 260: 114279.

784 Yılmaz S, Özgüner H, Mumcu S. An aesthetic approach to planting design in urban parks and greenspaces.
785 *Landscape Research* 2018; 43: 965-983.

786 Yu H, Zhu S, Liu Z. Influence of Urbanization on the Temperature Changes in Nanjing. *Ecology and*
787 *Environmental Sciences* 2014; 23: 1425-1431.

788 Yu Z, Chen T, Yang G, Sun R, Xie W, Vejre H. Quantifying seasonal and diurnal contributions of urban
789 landscapes to heat energy dynamics. *Applied Energy* 2020; 264: 114724.

790 Yu Z, Guo X, Jørgensen G, Vejre H. How can urban green spaces be planned for climate adaptation in
791 subtropical cities? *Ecological Indicators* 2017; 82: 152-162.

792 Zhang X, Zhong T, Feng X, Wang K. Estimation of the relationship between vegetation patches and urban
793 land surface temperature with remote sensing. *International Journal of Remote Sensing* 2009;
794 30: 2105-2118.

795 Zhang Z, Lv Y, Pan H. Cooling and humidifying effect of plant communities in subtropical urban parks.
796 *Urban Forestry & Urban Greening* 2013; 12: 323-329.

797 Zheng J-y, Yi Y-h, Li b-y. A new scheme for climate regionalization in China. *Acta Geographica Sinica* 2010;
798 65: 3-13 (in Chinese).

799 Zhou W, Qian Y, Li X, Li W, Han L. Relationships between land cover and the surface urban heat island:
800 seasonal variability and effects of spatial and thematic resolution of land cover data on
801 predicting land surface temperatures. *Landscape Ecology* 2014; 29: 153-167.

802 Ziter CD, Pedersen EJ, Kucharik CJ, Turner MG. Scale-dependent interactions between tree canopy cover
803 and impervious surfaces reduce daytime urban heat during summer. *Proceedings of the*
804 *National Academy of Sciences* 2019; 116: 7575.

805